Revisiting the influence of the scanning speed on surface topography and microstructure of IN718 thin walls in directed energy deposition additive manufacturing

Michèle Bréhier, Daniel Weisz-Patrault, Christophe Tournier

▶ **To cite this version:**

Michèle Bréhier, Daniel Weisz-Patrault, Christophe Tournier. Revisiting the influence of the scanning speed on surface topography and microstructure of IN718 thin walls in directed energy deposition additive manufacturing. 6th CIRP Conference on Surface Integrity, Jun 2022, Lyon, France. pp.470-476, 10.1016/j.procir.2022.03.074 . hal-03644083

HAL Id: hal-03644083
https://hal.science/hal-03644083v1

Submitted on 18 Apr 2022

HAL is a multi-disciplinary open access archive for the deposit and dissemination of scientific research documents, whether they are published or not. The documents may come from teaching and research institutions in France or abroad, or from public or private research centers.

L'archive ouverte pluridisciplinaire **HAL**, est destinée au dépôt et à la diffusion de documents scientifiques de niveau recherche, publiés ou non, émanant des établissements d'enseignement et de recherche français ou étrangers, des laboratoires publics ou privés.

Revisiting the influence of the scanning speed on surface topography and microstructure of IN718 thin walls in directed energy deposition additive manufacturing

Michèle Bréhier[a,b], Daniel Weisz-Patrault[b], Christophe Tournier[a,*]

[a] *Université Paris-Saclay, ENS Paris-Saclay, LURPA, 4 avenue des sciences, Gif-sur-Yvette 91190, France*
[b] *LMS - UMR CNRS 7649, École Polytechnique, Institut Polytechnique de Paris, Route de Saclay, Palaiseau 91120, France*

Abstract

Controlling the mechanical properties of metallic parts produced by additive manufacturing remains challenging. The mechanical behavior of parts is mainly related to the microstructure, which depends on process parameters and manufacturing strategies. The scanning speed is one of the key parameters that can be modulated during the process (according to the kinematic behavior of the machine tool) in order to reach different microstructures. Thus, in this work, an experimental study in laser metal powder directed energy deposition is conducted to analyze the influence of the scanning speed on the macroscopic geometry, the surface topography, and the microstructure. To do so, a series of single-layer experiments has been conducted to establish an empirical relationship between the laser power, the powder flow-rate and the scanning speed on the one hand, and the layer height and width on the other hand. In addition, six multi-layer thin-walled structures have been produced for various laser powers and scanning speeds in order to determine an association with macroscopic features, topography and microstructure. This approach opens interesting long-term perspectives to better control microstructures in DED.

Keywords: Laser cladding, surface topography, microstructure, scanning speed

1. Introduction

Additive manufacturing allows for the production of complex parts, and has been widely used for several years. Among the various processes of metal additive manufacturing, directed energy deposition (DED) is considered in this contribution, more specifically laser metal powder directed energy deposition (LMP-DED) also referred as laser metal deposition (LMD). Among all the process parameters, only three will be considered in this paper, namely: the scanning speed, the laser power, and the powder flow-rate. Mechanical properties of parts produced by metal additive manufacturing significantly depend on various aspects that should be monitored such as porosity [1], lack of fusion defects [2], residual stresses [3], etc. However, this paper mostly focuses on microstructures. Indeed, one of the main challenge to improve the process is to better control the microstructures, either to ensure homogeneity or on the contrary to purposely introduce targeted gradients. The microstructure commonly reported in the literature consists in elongated grains roughly oriented along the build direction with sometimes small equiaxed grains between each layer [4]. Several studies investigate how this standard microstructure is affected by changes of process parameters. For instance, Parimi et al. [5] showed that grain size and grain orientation depend on the linear energy, defined as the laser power divided by the scanning speed. By increasing the laser power, grains become larger and less tilted with respect

*Corresponding author. Tel.: +33-1-81-87-51-84. *E-mail address:* christophe.tournier@ens-paris-saclay.fr

to the build direction. In case of high linear energy, continuous grains through the layer interfaces are reported. Cao et al. [6] studied the influence of overlap rate on grain width by imposing 20 to 50% variations. Guévenoux et al. [7] compared electron back-scatter diffraction (EBSD) maps with and without dwell time between each layer. Dwell time has been found to be associated with a finer grain structure and stronger crystallographic texture. There are many possible scanning strategies in AM, the most commonly used are unidirectional or zigzag trajectories as they are easy to implement. However, they can lead to poor surface quality on the edges that are not parallel to the deposition path. To overcome this difficulty, contour or hybrid strategies can be considered. Ribeiro et al. [8] compared raster, zigzag, chessboard and spiral strategies and showed that the deposition strategy not only impact flatness and roughness, but also porosity and microstructures. Regardless of the scanning strategy, the problem of speed variations undergone during the process must also be addressed. Duong et al. [9] showed that the programmed scanning speed is not always respected, especially on turning points and when the machine stops and starts to stay synchronized with the laser state. Machine kinematics leads to unwanted speed variations of the nozzle, which could have an impact on the microstructure. Thus, the scanning speed, which can evolve along the scanning path is a parameter whose influence on the microstructure must be controlled. Moreover, beyond the LMD process, the variability of the scanning speed, programmed or experienced, is a transverse problem for all the DED processes.

The first objective of this preliminary work is to study the range of scanning speeds for which the part can be manufactured until its completion. Indeed, the scanning speed has a significant impact on the layers size and shape, and thus on parts topography. Due to possible melt pool instabilities, all sets of process parameters (i.e., laser power, scanning velocity, and powder flow rate) do not ensure the production of continuous layers. It is therefore necessary to conduct single-layer experiments to define -for a given material and machine- a parameter domain in which proper continuous layers are obtained. In addition, a quantitative relationship between process parameters and layer size can be determined, as detailed in section 2.

The second objective is to manufacture and analyze a series of single-track multi-layer thin-walled structures to determine an association between process parameters on the one hand and macroscopic features, topography and microstructure on the other hand. Specimen fabrication is detailed in section 3. In particular, for each set of process parameters, the Z-increment is adjusted with respect to the expected layer height obtained from the single-layer experiments. In addition, for different combinations of scanning speeds and laser powers, an analysis of surface quality, topography and microstructure is carried out in section 4.

Thus, this study contributes to a longer-term objective consisting in fine-tuning process parameters in order to reach targeted microstructures.

2. Influence of scanning speed on layer size

All single-layer experiments and thin walls were made on a 5-axis BeAM™ Mobile machine equipped with a type 10Vx nozzle and a 500 W fiber laser source from IPG™ with an operational range of 200-400 W for this nozzle. The powder used was Inconel 718. The first step is to determine the parameter range within which laser claddings are satisfying. The experimental design was defined around the operating point: laser power of 245 W, scanning speed of 1800 mm/min and powder flow-rate of 9 g/min. Thus, three powder flow-rates (7, 9 and 11 g/min), six laser powers (225, 250, 275, 300, 325, 350 W) and five scanning speeds (1125, 1500, 1875, 2250, 2625 mm/min) have been tested, resulting in 90 single-layer experiments as shown in figure 1. Although all the claddings were successfully made, their shapes and sizes significantly depend on process parameters. A focus variation microscope IF-SensorR25 from Alicona™ was used to measure the height and width of each layer. To do so, an optical element points to a sample and searches the best focus position in order to estimate the depth. The layer height and width respectively denoted by H and W were measured using this method to determine an empirical law relating H and W with the laser power P, the scanning velocity V and the powder flow-rate Q. Results are reported in table 1 and compared to the literature [10, 11]. As reported in the literature, the influence of the powder flow-rate on the layer width is negligible compared to the scanning speed and the laser power. Similarly, the layer height is almost inversely proportional with respect to the scanning speed, in good agreement with the literature. However, the influence of the laser power seems more significant than the powder flow-rate, unlike previous studies.

This discrepancy could be explained by the fact that the experiments were not identical. De Oliveira et al. [10] used a graded experiment, continuously increasing the laser power along each of the 25 tracks performed with the

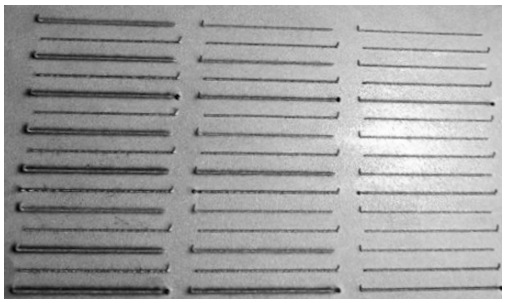

Figure 1: Part of the claddings on the base plate.

Table 1: Layer height H and width W as a function of laser power P, scanning speed V, and powder flow-rate Q, and comparison with other studies.

	Height H	Width W
Present study	$P^{0,44}\,V^{-0,90}\,Q^{0,26}$	$P^{0,61}\,V^{-0,37}\,Q^{0,068}$
De Oliveira et al. [10]	$V^{-1}\,Q$	$P\,V^{-0,5}$
El Cheikh et al. [11]	$P^{0,25}\,V^{-1}\,Q^{0,75}$	$P^{0,75}\,V^{0,25}$

nickelchromium based alloy powder 19E Sulzer-Metco™ . The empirical law proposed by El Cheikh et al. [11] is based on a 27-tracks experiment with 316L stainless steel. The number of claddings realized as well as the range of variation of the parameters, the material and the substrate could influence the interpolation law based on the experiments.

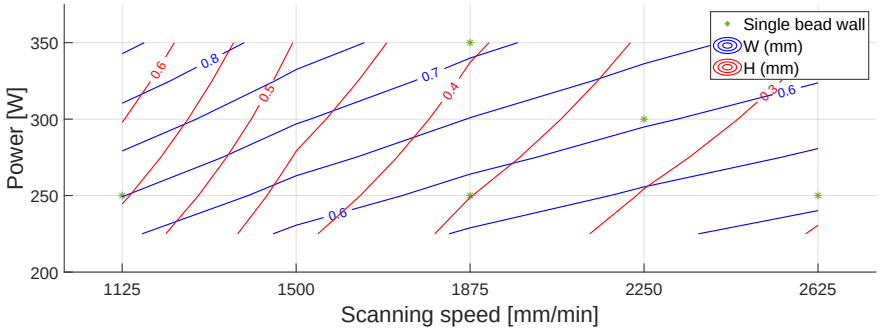

Figure 2: Isoparametric curves of layer height H and width W as a function of laser power P and scanning speed V.

Based on the proposed empirical law, isoparametric curves representing the layer height and width as a function of the laser power and the scanning speed are presented in figure 2 for a given powder flow-rate. When manufacturing more complex parts, the turns in the laser trajectory induce slowdowns of the machine tool owing to its own kinematics. However, the proposed empirical law shows that the laser power cannot be adjusted as the scanning speed changes to keep uniform the layer height and ensure a homogeneous layer stacking. Indeed, the isoparametric curves presented in figure 2 suggest that for a given layer height the appropriate laser power range is not wide enough to compensate significant scanning speed variations. Nevertheless, the dynamic evolution of the layer size according to non-constant laser speed should be investigated for various accelerations, and is being considered for further work.

3. Multi-layer thin walls

3.1. Design of experiments

Thin walls experiments were designed on the basis of previous single-layer experiments. Thus, a single powder flow-rate $Q = 9$ g/min has been considered for all thin walls experiments, as this parameter has a negligible influence. In addition, since all claddings were satisfying, the entire ranges of laser powers P and scanning speeds V have been considered in order to test significantly different manufacturing conditions. More precisely, a total of six 40 mm long and 30 mm high thin walls have been produced according to the experimental design presented in figure 3. Three sets of walls with increasing scanning speeds can be identified: two sets with constant laser power (i.e., 250 W for walls 1, 4 and 6 and 350 W for walls 3 and 5), and one set with constant linear energy (i.e., 8 J/mm for walls 1, 2 and 3). In addition, all experiments were conducted with a unidirectional scanning strategy on the same build platform. For each wall, a 0.5 s dwell time was applied between each layer. As already mentioned, the Z-increment was adapted for each wall and set to the layer height of the corresponding single-layer experiment minus 0.03 mm. The final height of the walls is within 4% of their theoretical values (i.e., number of layers multiplied by the layer height), which supports the choice of the Z-increment.

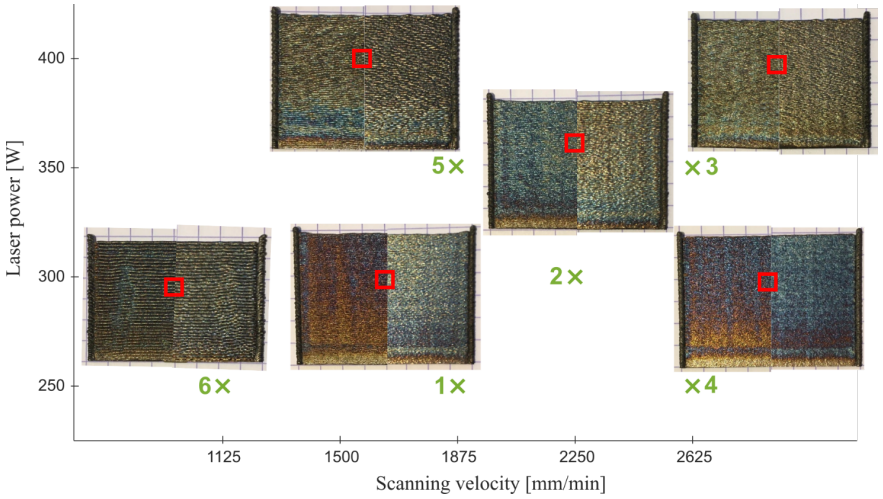

Figure 3: Experimental design in the P, V diagram (i.e., green cross markers). Both sides of the corresponding pictures are presented (i.e., front side on the left and back side on the right), and red square markers correspond to the magnification zone presented in figure 4.

3.2. Macroscopic analysis

Although the six walls were successfully stacked, significant differences can be noticed in figure 4. Thus, three types of stacking are distinguished: layers properly aligned on top of each other for wall 1 and wall 4, staggered stack for wall 2 and wall 6 and complex stacking suggesting instabilities of the melt pool corresponding to the highest laser power for wall 3 and wall 5.

4. Surface characterization

4.1. Topography analysis

For both sides of each wall, the surface topography was measured using the microscope IF-SensorR25. Measurements were carried out in five different areas (i.e., center, top and bottom on the vertical centerline, and left and right on the horizontal centerline). Considering the surface anisotropy characterized by a quasi-periodic profile that is

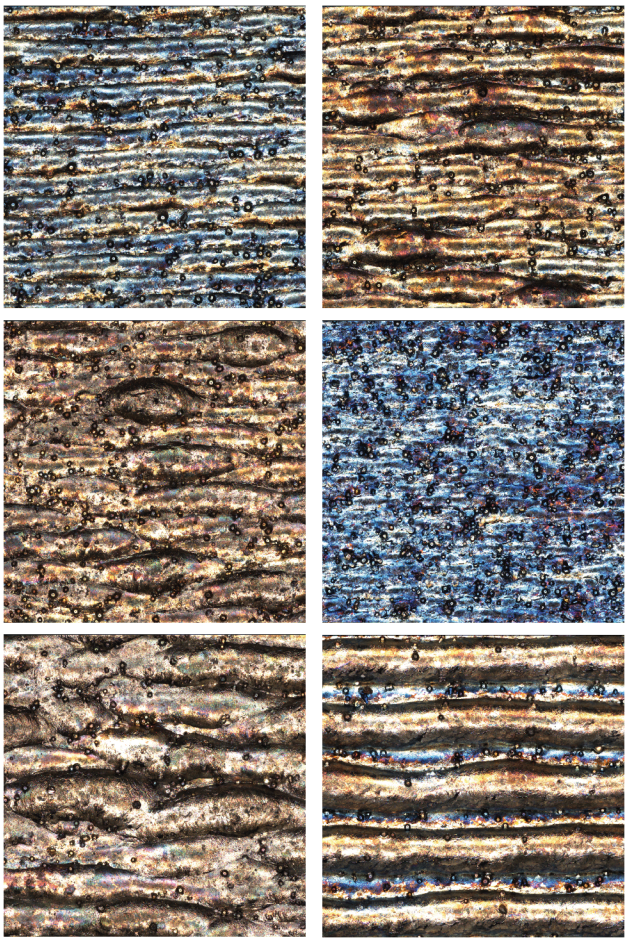

Figure 4: Stacking of the different walls (arranged as follows 1-2;3-4;5-6). All pictures have the same scale (i.e., 3.5 mm $\times$ 3.5 mm), and are extracted in the center area of the back side.

usually obtained in LMD, the following parameters on the primary (ISO 3274:1996) and roughness (ISO 4287:1997) profiles were evaluated:

- Arithmetical mean height (Pa, Ra)
- Mean height of the profile elements (Pc, Rc)
- Mean width of the profile elements (PSm, RSm)

Thus, the mean height of the profile elements is related to the layer width, whereas the mean width of the profile elements is related to the layer height. Each parameter was evaluated along a profile in each of the five measurement zones to extract the average value for both sides (i.e., front and back), as listed in table 2. In figure 5, the primary profile exhibits the shape of the overlaying layer, whereas the roughness profile emphasizes the valley between layers. The values of the primary profile parameters as a function of the process parameters (i.e., laser power and scanning speed) are shown in figure 6. It can be observed that the primary profile parameters are higher on the front side than on the back side. This is visually confirmed by the higher density of unmelted powder particles on the front side than on the back side. This is probably due to a misalignment of the inert gas flow carrying the powder towards the front side. Apart from this difference whose magnitude is almost constant, a significant positive linear correlation can be observed between the parameters Pa, Pc and PSm and the laser power. However, for the scanning speed, the correlation is much weaker or even non significant.

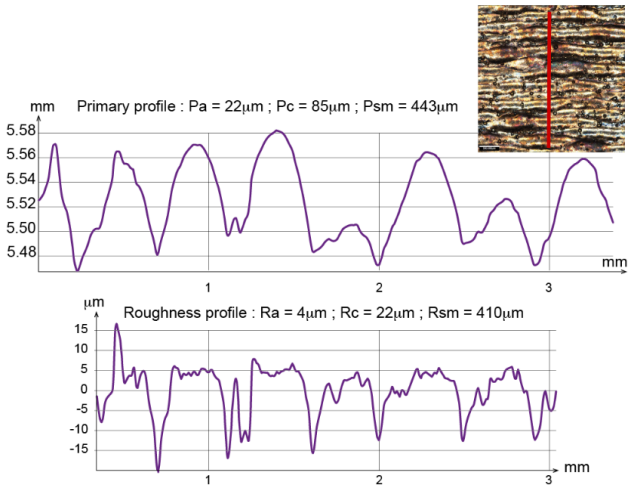

Figure 5: Primary and roughness profiles of "wall 2 back side" (center area)

Table 2: Resulting surface roughness parameters for both sides of the walls (f: front and b: back).

	Power W	Speed m/min	Pa μm	Pc μm	PSm μm	Ra μm	Rc μm	RSm μm
Wall 1.f	250	1875	22.2	79.6	**388**	7.1	32.5	265
Wall 1.b	250	1875	15.4	60.4	462	6.2	29.5	290
Wall 2.f	300	2250	27.2	101	**926**	**7.6**	40.0	313
Wall 2.b	300	2250	19.6	70.6	610	**4.4**	**21.0**	330
Wall 3.f	350	2625	34.4	119	735	7.0	40.8	356
Wall 3.b	350	2625	28.8	100	704	6.4	**41.4**	**399**
Wall 4.f	250	2625	13.4	53.0	514	6.4	28.2	**222**
Wall 4.b	250	2625	**12.0**	**49.4**	473	5.4	25.4	260
Wall 5.f	350	1875	**46.0**	**143**	871	6.6	37.4	357
Wall 5.b	350	1875	36.6	123	770	5.0	25.0	385

Regarding roughness parameters (figure 7), the correlation with the laser power is obvious for RSm (i.e., mean width of the profile elements) for both sides. The correlation is more moderate for Rc (i.e., mean height of the profile elements) and null for Ra. Once again, there is no significant correlation between these three parameters and the scanning speed. Thus, in the chosen parameter domain, it seems that the scanning speed has very little influence on the topography of the produced walls compared to the laser power.

4.2. Microstructure analysis

Samples were extracted from the walls and prepared by mirror polishing and electrolytic etching with orthophosphoric acid in order to analyze the microstructures with an optical microscope. The different layers were clearly identifiable for all samples. Thus, by comparing the photographs of the wall surfaces and the corresponding micrographs, the layers identified on the micrographs can be superimposed on those directly visible on the walls as shown in figure 8. Good agreement is observed for the layer size and the non-regular layer shape of walls 3 and 5. The comparison is relevant despite surface polishing, which flattens specimens, because surface polishing is shallow.

The expected dendritic structure is revealed with higher magnification. For instance, the dendritic structure of wall 1 (i.e., P=250 W, V=1875mm/min) is presented at two different locations of the specimen in figure 9. Long dendrites, roughly oriented along the build direction, are separated by small grains between the layers. On the right side of the figure, the dendrites appear to cross two layers. This occasional pattern is not prevailing in the wall and

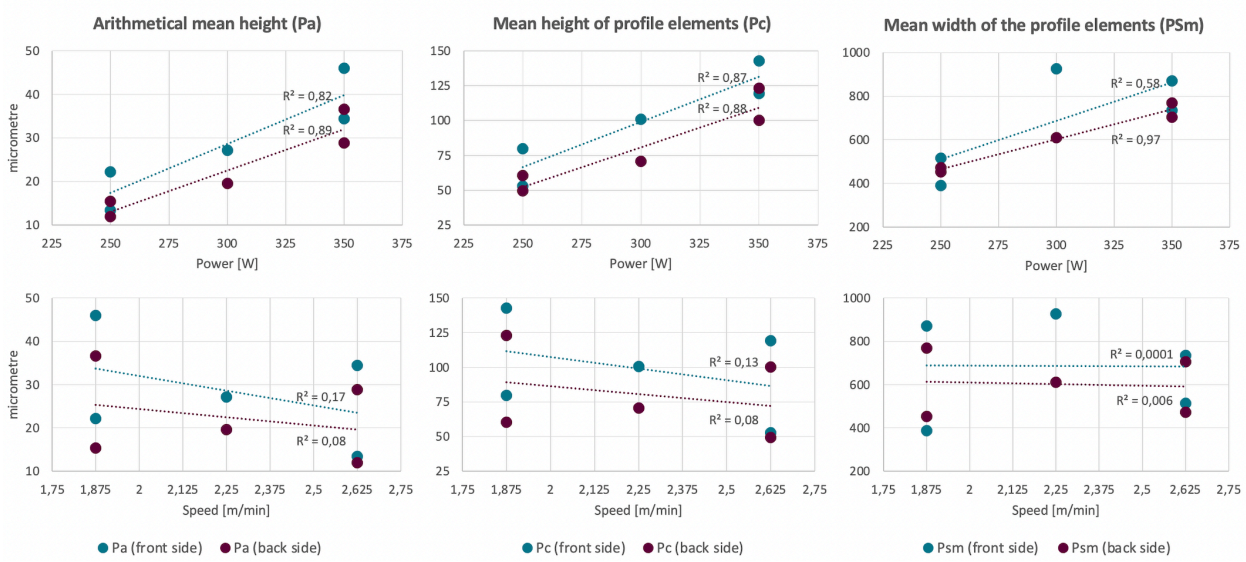

Figure 6: Primary profile parameters versus scanning velocity and power

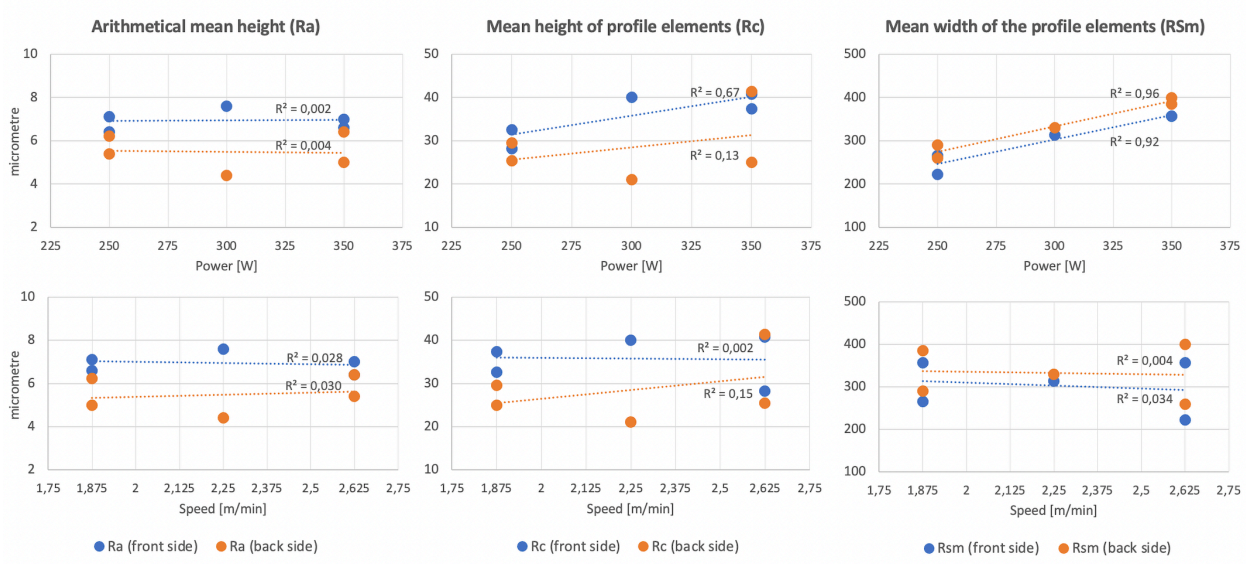

Figure 7: Roughness profile parameters versus scanning velocity and power

is always limited to two successive layers. In addition, black spheres are visible and correspond to gas porosities (20-60 µm) and porosities related to powder quality (10 µm).

To evaluate -all things being equal- the influence of the scanning speed on the microstructure, walls 4 (P=250 W, V=2625 mm/min) and 6 (P=250 W, V=1125 mm/min) were compared, as shown in figure 10. For wall 6, with the smallest scanning speed and thus the largest linear energy, layers are more distinct, the dendrite orientations are much more regular, and do not seem to cross the layers. For wall 4, statistical dispersion of dendrite orientations is more significant even though dendrites roughly align along the print direction. In addition, for wall 4 some dendrites seem to be continuous through two successive layers, whereas this pattern was not observed for wall 6 with the largest linear energy. The latter observation is not in agreement with Parimi et al. [5], which report that larger linear energy is associated to continuous grains through successive layers. This can be explained by the 0.5 s dwell time between each

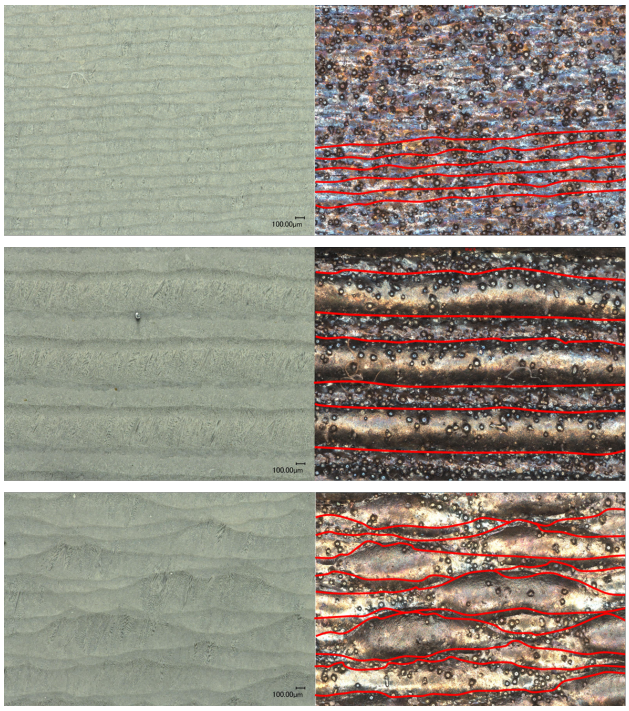

Figure 8: Comparison between microstructure and topography for the 3 types of stacking: alignment on top of each other (wall 4), staggered (wall 6), and complex pattern (wall 5)

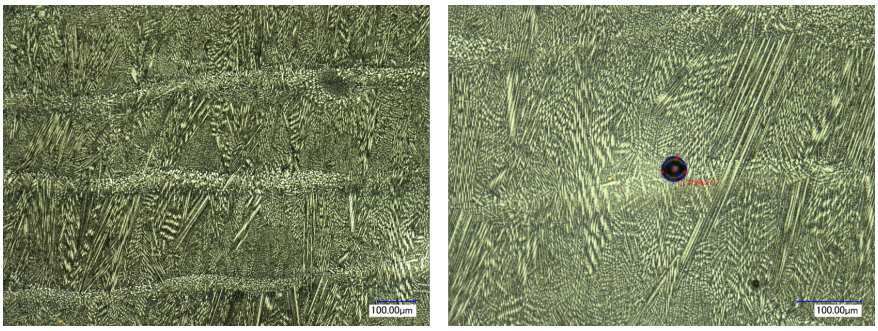

Figure 9: Micrographs showing the dendritic structure of wall 1 (i.e., P=250 W, V=1875 mm/min).

layer as well as the unidirectional scanning strategy, which both allows the previous layer to cool down before adding a new one. Thus, considering the chosen scanning strategy and dwell time, the proposed experiments did not allow to produce significantly different dendrite orientation distributions and grain morphologies despite the wide range of parameters that has been tested. However, very different stacking typologies have been obtained, which determine not only grain size but also spatial distribution of long dendrites with respect to smaller grains.

5. Conclusions

Modulating process parameters, such as the scanning speed during the construction of parts in LMP-DED is of great interest. However, this modulation impacts all stages of the process. First, from a geometrical point of view, the scanning speed modulation modifies the morphology of single layer and multi-layer thin walls. Therefore, empirical laws were derived for the layer width and height for a range of admissible process parameters (i.e., scanning speed,

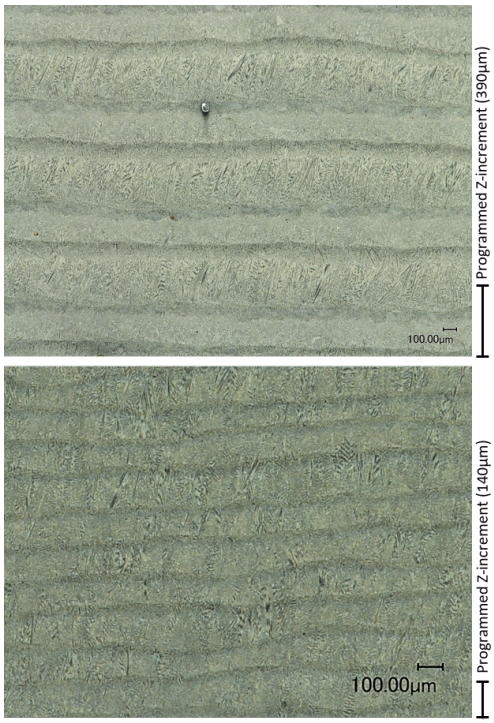

Figure 10: Micrographs of wall 6 (P=250 W, V=1125 mm/min) and wall 4 (P=250 W, V=2625 mm/min).

laser power and powder flow-rate). Each production system and powder batch being specific, these empirical laws are slightly different from those published in the literature. Based on these results, a design of experiments was proposed to study the manufacturing of single-track multi-layer thin walls from macroscopic, topographic and microstructural points of view. If the influence of the scanning speed seems significant at the macroscopic level, the influence on microstructures seems mostly related to the different layer stacking typologies, at least in the studied parameter range. A more detailed study of the microstructures using EBSD analyses is in progress and should provide more information. It also seems necessary to explore higher linear energy levels.

Acknowledgements

This work is part of the MIFASOL project and is supported by a grant overseen by the French National Research Agency (ANR-20-CE10-0009).

References

[1] M. Montazeri, A. R. Nassar, A. J. Dunbar, P. Rao, In-process monitoring of porosity in additive manufacturing using optical emission spectroscopy, IISE Transactions 52 (2020) 500–515.

[2] P. Margerit, D. Weisz-Patrault, K. Ravi-Chandar, A. Constantinescu, Tensile and ductile fracture properties of as-printed 316l stainless steel thin walls obtained by directed energy deposition, Additive Manufacturing 37 (2021) 101664.

[3] D. Weisz-Patrault, P. Margerit, A. Constantinescu, Residual stresses in thin walled-structures manufactured by directed energy deposition: in-situ measurements, fast thermo-mechanical simulation and buckling., Additive Manufacturing (2022 (submission)).

[4] Y. Balit, E. Charkaluk, A. Constantinescu, Digital image correlation for microstructural analysis of deformation pattern in additively manufactured 316l thin walls, Additive Manufacturing 31 (2020) 100862.

[5] L. L. Parimi, G. Ravi, D. Clark, M. M. Attallah, Microstructural and texture development in direct laser fabricated in718, Materials Characterization 89 (2014) 102–111.
[6] J. Cao, F. Liu, X. Lin, C. Huang, J. Chen, W. Huang, Effect of overlap rate on recrystallization behaviors of laser solid formed inconel 718 superalloy, Optics & Laser Technology 45 (2013) 228–235.
[7] C. Guévenoux, S. Hallais, A. Charles, E. Charkaluk, A. Constantinescu, Influence of interlayer dwell time on the microstructure of inconel 718 laser cladded components, Optics & Laser Technology 128 (2020) 106218.
[8] K. S. Ribeiro, F. E. Mariani, R. T. Coelho, A study of different deposition strategies in direct energy deposition (ded) processes, Procedia Manufacturing 48 (2020) 663–670.
[9] T.-Q. Duong, N. Ferrier, S. Lavernhe, C. Tournier, A kinematic simulation software for additive manufacturing metal deposition processes, in: ICWAM'19, International Congress On Welding, Additive Manufacturing And Associated Non Destructive Testing.
[10] U. De Oliveira, V. Ocelik, J. T. M. De Hosson, Analysis of coaxial laser cladding processing conditions, Surface and Coatings Technology 197 (2005) 127–136.
[11] H. El Cheikh, B. Courant, J.-Y. Hascoët, R. Guillén, Prediction and analytical description of the single laser track geometry in direct laser fabrication from process parameters and energy balance reasoning, Journal of materials processing technology 212 (2012) 1832–1839.